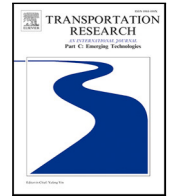Contents lists available at ScienceDirect

Transportation Research Part C

journal homepage: www.elsevier.com/locate/trc

Overview Paper

Dispatching a fleet of electric towing vehicles for aircraft taxiing with conflict avoidance and efficient battery charging

Simon van Oosterom [a],[*], Mihaela Mitici [b], Jacco Hoekstra [a]

[a] *Faculty of Aerospace Engineering, Delft University of Technology, Kluyverweg 1, HS 2926 Delft, The Netherlands*
[b] *Faculty of Science, Utrecht University, Heidelberglaan 8, 3584 CS Utrecht, The Netherlands*

ARTICLE INFO

ABSTRACT

Following the Paris Accords, the aviation industry aims to become climate neutral by 2050. In this line, electric vehicles that tow aircraft during taxiing are a promising emerging technology to reduce emissions at airports. This paper proposes an end-to-end optimization framework for electric towing vehicles (ETVs) dispatchment at large airports. We integrate the routing of the ETVs in the taxiway system where minimum separation distances are ensured at all times, with the assignment of these ETVs to aircraft towing tasks and scheduling ETV battery recharging. For ETV recharging, we consider a preemptive charging policy where the charging times depend on the residual state-of-charge of the battery. We illustrate our model for one day of operations at a large European airport. The results show that the 913 arriving and departing flights can be towed with 38 ETVs, with battery charging distributed throughout the day. The fleet size is shown to increase approximately linear with the number of flights in the schedule. We also propose a greedy dispatchment of the ETVs, which is shown to achieve an optimality gap of 6% with respect to the number of required vehicles and with 22% with respect to the maximum delay during towing. We also show that both algorithms can be leveraged to account for flight delays using a rolling horizon approach, and that over 95% of the flights can be reallocated if delays occur. Overall, we propose a roadmap for ETV management at large airports, considering realistic ETV specifications (battery capabilities, kinematic properties) and requirements for aircraft collision avoidance during towing.

1. Introduction

Striving to meet the climate-neutrality targets set by the Paris Accords (European Commission, 2016) and the Glasgow Climate Pact (UNFCCC, 2021), the aviation industry aims for net-zero emissions by 2050 (IATA, 2021; Shepardson, 2021). To achieve this, one of the objectives is to reach zero-emission ground-based aviation activities. In fact, the Netherlands and Australia aim to achieve this objective by 2030 (Schiphol, 2019a; Sydney Airport, 2021).

Aircraft taxiing is one of the main contributors to ground-based emissions (Khadilkar and Balakrishnan, 2012; Lukic et al., 2019). In fact, aircraft taxiing accounts for 54% of the total emissions associated with the landing/take-off cycle (Camillere and Batra, 2021). As an example, studies at Heathrow airport have shown that 56% of the total nitrogen-oxides emissions are due to taxiing aircraft (Dzikus et al., 2011). Also, on-ground fuel consumption has been estimated to be as high as 7% of the average of the total flight fuel consumption (Khadilkar and Balakrishnan, 2012; Nikoleris et al., 2011). To meet climate-neutrality targets for aviation, there is an urgent need for new technologies and procedures to reduce emissions during aircraft taxiing.

---

* Corresponding author.
    E-mail address: s.j.m.vanoosterom@tudelft.nl (S. van Oosterom).

Electric vehicles that tow aircraft between runways and gates are seen as a key enabling technology for emissions reduction. Preliminary studies have shown that employing hybrid-electric vehicles for aircraft towing already reduces the CO_2 emissions during taxiing by 82% (Camillere and Batra, 2021). A full Electric Towing Vehicles (ETV) is expected to further reduce emissions during taxiing. Dispatching ETVs to tow aircraft is, however, a challenging logistic problem for which two main aspects need to be addressed: (1) algorithms are needed to efficiently allocate ETVs to tow aircraft and to recharge ETVs' batteries, and (2) algorithms are needed to route the aircraft towed by ETVs such that a minimum separation distance between any two towed aircraft is maintained at all times, such that collisions are avoided. To the best of our knowledge, a framework for ETV dispatching that fully addresses these aspects in an integrated way is lacking. Routing algorithms for ETVs enable a safe and efficient management of the airport ground movements, yet the availability and capabilities of ETVs for routing is inherently dependent on the ETVs' charging schedules and on the actual allocation of ETVs to aircraft. Reversely, an efficient allocation of ETVs for charging and aircraft towing tasks is dependent on the routing of the ETV-towed aircraft in the taxiway system. In this paper, we propose to address the two logistic aspects in one integrated framework.

The dispatching of a generic vehicle fleet has frequently been posed in existing literature as a vehicle routing problem with time windows (VRP-TW). The VRP-TW problem requires that a fleet of vehicles is scheduled to visit a set of customers within a given time window (see Bräysy and Gendreau, 2005a,b). Often considered objectives for the VRP-TW problem are the minimization of transport costs (Taş et al., 2014), traveled distance (Savelsbergh, 1992), or the size of the fleet of vehicles (Figliozzi, 2010).

For generic electric vehicles which have battery charging requirements, solutions to the Electric-VRP-TW (E-VRP-TW) problem have been proposed. Initial studies assume a recharging policy where each visit of an electric vehicle to a recharging station takes a fixed amount of time, and the battery is charged to full capacity. During this re-charging time, the vehicles cannot visit customers. Conrad and Figliozzi (2011) propose an iterative construction algorithm to minimize the required number of vehicles. Erdoğan and Miller-Hooks (2012) propose a density-based clustering algorithm (DBCA) heuristic which minimizes the traveled distance. Omidvar and Tavakkoli-Moghaddam (2012) propose a genetic algorithm (GA) which minimizes the transportation cost of the fleet of electric vehicles.

Further studies (Schneider et al., 2014; Hiermann et al., 2016) extend the E-VRP-TW problem by considering a battery recharge time which depends on the residual state-of-charge of the battery. Here also, the batteries are charged to full capacity every time. In Schneider et al. (2014) a tabu search (TS) algorithm is developed to minimize the traveled distance. Hiermann et al. (2016) propose an adaptive large neighborhood search (ALNS) heuristic which minimizes the required fleet size. Compared to the E-VRP-TW problems with fixed charging times, as in earlier studies (Erdoğan and Miller-Hooks, 2012; Omidvar and Tavakkoli-Moghaddam, 2012; Conrad and Figliozzi, 2011), tests on the VRP-TW Solomon instances (Solomon, 1987) by Schneider et al. (2014) have shown that this charging assumption leads to a decrease in transportation costs of up to 10%. Building on this, an extension of the E-VRP-TW problem is proposed, where the recharging time not only depends on the residual state-of-charge of batteries, but partial charging of these batteries is also allowed (Desaulniers et al., 2016; Keskin and Çatay, 2016; Lin et al., 2021). Desaulniers et al. (2016) consider the minimization of the traveled distance and develop a branch price & cut (BPC) algorithm to solve the problem to optimality. Keskin and Çatay (2016) and Lin et al. (2021) respectively develop an ALNS and a variable neighborhood search (VNS) heuristic to minimize the transport costs. Keskin and Çatay (2016), demonstrate that their model is able to further decrease transport costs with up to 5%, when applied on the Solomon instances.

When applied to the dispatching of ETVs for aircraft towing, the E-VRP-TW problem is only considered with simple battery charging policies such as fixed charging times. In Soltani et al. (2020), ETVs are assumed to have an infinite battery life, i.e., no charging is required for these ETVs throughout the day of operations. Thus, this problem reduces to a general vehicle VRP-TW. Specific to ETVs, the authors ensure that the routing of the towing ETVs is done such that the towed aircraft do not collide with each other, by ensuring a minimum separation distance between any two ETVs. The proposed model is applied at Montreal International Airport on a schedule with 215 flights. Realistic ETV specifications (Lukic et al., 2019), however, show that the capacity of the ETV batteries are limited and that multiple battery recharging moments are expected throughout a day of operations. These are unaccounted for by Soltani et al. but will impact the availability of the ETVs, and hence their schedule.

Baaren and Roling (2019) consider the E-VRP-TW problem where ETVs take a fixed amount of time to recharge their batteries to full capacity, irrespective of the remaining state-of-charge of the battery. In contrast to Soltani et al. van Baaren and Roling do not ensure a minimum separation distance between towing ETVs as a part of the ETV dispatchment problem. The model is applied at Amsterdam Airport Schiphol for 1230 arriving and departing aircraft that are towed with ETVs. However, as presented in the previous paragraph, the constant-time battery recharging assumption has been shown to result in a lower vehicle fleet utilization when compared to the models with state-of-charge dependent recharge times (Keskin and Çatay, 2016).

In this paper we propose a two-phase mixed integer linear program to dispatch a fleet of ETVs at a large airport during a full day of operations. We propose an *integrated* approach by considering both the routing of towing ETVs across the taxiways, as well as the scheduling of ETVs for aircraft towing and battery recharge. Our model ensures that, while towing, the ETVs (and aircraft) maintain a minimum separation distance. Sequentially, our model assigns ETVs to towing tasks while taking into account the need of ETVs to recharge their batteries. The charging schedule is based on a preemptive charging policy and considers the residual state-of-charge of the batteries.

We illustrate our method for one day of operations at Amsterdam Airport Schiphol (AAS). A total of 913 arriving and departing flights are considered for towing throughout the day. These flights are operated by a mix of narrow-body, wide-body and heavy-wide-body aircraft, each with its own designated ETV type. The results show that a fleet of 38 ETVs in required to tow these aircraft for a total average of 4 h. Also, the battery recharge moments for these ETVs are distributed throughout the day, with a maximum demand for charging in the period 17:00–19:00, i.e. just before the peak evening hours at the airport. To further support
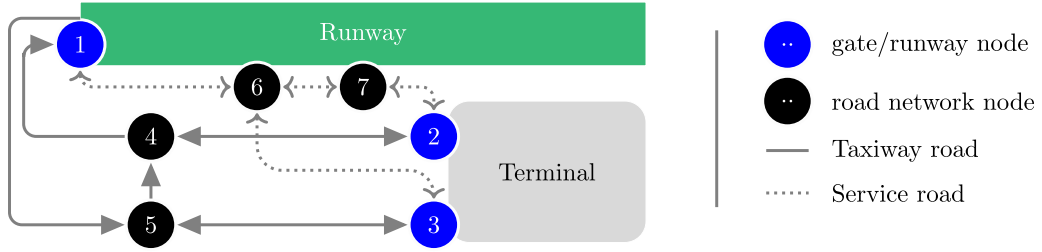
Fig. 1. Example of an airport taxiway and service road network. The runway entrance and exit is located at node 1, and the gates are located at nodes 2 and 3. The taxiway is shown with *solid* lines, while the service roads are shown in *dashed* lines, while traffic directions are indicated with arrowheads. In this example: $N^R = \{1\}$, $N^G = \{2, 3\}$, $N_X = \{4, 5\}$, and $N_S = \{6, 7\}$, such that: $E_X = \{(5, 4)\}$, $E_X^G = \{(2, 4), (4, 2), (3, 5), (5, 3)\}$, $E_X^R = \{(1, 5), (4, 1)\}$, $E_S = \{\{6, 7\}\}$, $E_S^G = \{\{2, 7\}, \{3, 6\}\}$, and $E_S^R = \{\{6, 1\}\}$.

the management of ETV in practice, we also propose a simple, Greedy ETV Fleet Dispatchment (GEFD) algorithm. GEFD reduces the computational time 50-fold in our case study at AAS, compared with our proposed mixed integer linear program, with an optimality gap of 5%.

The main contributions of the paper are:

(i) We propose an end-to-end management framework for ETVs that integrates the routing of the ETVs in the taxiway system with the scheduling of these ETVs for aircraft towing and battery re-charging;

(ii) We include a partial battery recharging policy for ETVs, which is identified as a research gap (Baaren and Roling, 2019);

(iii) We propose a Greedy heuristic for ETV management, which is shown to achieve an optimality gap of 5% relative to our optimal solutions.

The remainder of this paper is organized as follows. In Section 2 we introduce the ETV dispatching problem taking. We then propose a model for the energy consumption and recharging rates of the ETVs in Section 3. In Section 4 we develop our ETV dispatchment optimization models. In Section 5 we illustrate our problem for one day of operations at Amsterdam Airport Schiphol. We compare the performance of our models with the performance of our proposed GEFD heuristic in Section 6. Finally, concluding remarks and future research directions are given in Section 7.

2. Problem description

We consider an airport where each day, the dispatching of an ETV fleet has to be optimized. While using ETVs to tow aircraft across the taxiways, collisions have to be avoided. During the day, these ETVs may also need to re-charge their batteries. An overview of all the used notation can be found in Table A.7.

2.1. Airport taxiways and service road networks

Let N_R be the set of runway entrance and exit nodes, and let N_G be the set of gates. These sets are connected by two networks. First we consider the directed graph $G_X = (N_X, E_X)$, the taxiway network which consists of junctions N_X and taxiway roads E_X. The taxiway is connected to the runways and gates via edges $E_X^G \subseteq N_X \times N_G$ and $E_X^R \subseteq N_X \times N_G$. Let $d_X : E_X \cup E_X^G \cup E_X^R \to \mathbb{R}^+$ and $v_X : E_X \cup E_X^G \cup E_X^R \to \mathbb{R}^+$ denote the length of – and maximum speed on – an edge of network G_X. The aircraft are assumed to be attached to an ETV while on G_X. When ETVs are not towing an aircraft, then these use a service road network to traverse the airport. This is represented by the undirected graph $G_S = (N_S, E_S)$, with E_S the set of service roads and N_S the set of junctions of the service roads. The service roads are connected to the runways and gates via edges $E_S^G \subseteq N_S \times N_G$ and $E_S^R \subseteq N_S \times N_G$. Let $d_S : E_S \cup E_S^G \cup E_S^R \to \mathbb{R}^+$ denote the length of an edge d_S of network G_S. On all edges of G_S, a maximum speed of v_S is in place. Fig. 1 shows an example of G_X and G_S at an airport.

2.2. Towing tasks

Let T denote a day of operations at the airport, such that $|T| = 24$ h. Let A be the set of aircraft which arrive or depart at the airport during T. Each aircraft from A represents a towing task: it needs to taxi from a node in N^R to one in N^G or vice versa. A towing task is defined as a tuple (n^s, t^s, n^e, m), where n^s is the node from where the task is started, $n^s : A \to N^R \cup N^G$, t^s is the first moment when this towing task can start, $t^s : A \to T$, and n^e the destination node for the aircraft, $n^e : A \to N^R \cup N^G$. Finally, $m : A \to \mathbb{R}^+$ is the mass of the aircraft.

The aircraft are categorized into three weight classes $W = \{NB, WB, H\text{-}WB\}$, denoting narrow-body, wide-body and heavy-wide-body aircraft, and into arriving and departing flights. Let $A^{arr,w}$ and $A^{dep,w}$ denote the arriving and departing aircraft of weight class $w \in W$, respectively. Finally, let $A^w := A^{arr,w} \cup A^{dep,w}$.
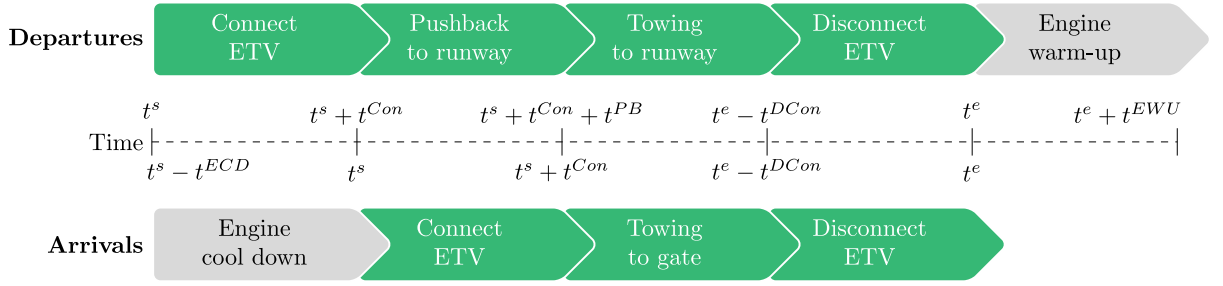
Fig. 2. Towing process for a departing/arriving aircraft. The ETV is connected to the aircraft in the time period $[t^s, t^e]$, marked by the green, darker, fields. (For interpretation of the references to color in this figure legend, the reader is referred to the web version of this article.)

2.3. ETV towing process

We assume the following ETV towing process (see Fig. 2). A departing aircraft $a \in A^{dep,w}$ is first connected to an ETV at a gate node $n^s(a)$, which takes t^{Con} time units. The aircraft is then pushed back onto the taxiway system G_X. Let t^{PB} denote the duration of this push-back. The aircraft is towed across G_X up to the runway entrance node $n^e(a)$. Finally, the aircraft and the ETV are disconnected, which takes t^{DCon} time. After this, the aircraft engine is warmed-up for t^{EWU} time and it proceeds to take-off.

In the case of an aircraft arrival at the airport, following landing, the aircraft's engine is first cooled down before it is attached to an ETV. Cooling down the engines takes t^{ECD} time.

2.4. ETV specifications

We assume a dedicated type of ETV to service each aircraft weight class $w \in W$. Whether in reality ETVs will be able to tow aircraft from smaller weight classes is not known at this moment, it may e.g. be hindered by incompatible mechanical couplings. Each type of ETV is equipped with a battery of capacity Q_w, has a mass of m_w, and a top-speed of v_w. We assume that on the service roads, ETVs drive at velocity v_S. When towing an aircraft across the taxi system G_X, the ETV's velocity is limited by v_w, and ETVs traverse an edge $e \in E_X$ at a constant velocity between a maximum $v_{max}^w(e) = \min\{v_X(e), v_w\}$ and a minimum $v_{min}^w : (E_X \cup E_X^G \cup E_X^R) \to \mathbb{R}^+$. In short, the minimum and maximum velocity for towing is defined for each edge in G_X and for a given type of aircraft. Besides, an aircraft is allowed to accelerate and decelerate at a maximum rate of a^{max}. Finally, let P_w denote the energy required to drive an ETV per unit time, where P_w is a function of the weight of the aircraft being towed and the ETV's velocity.

2.5. Routing and separation distance policy

We assume the following routing policy for aircraft and ETVs traversing G_X and G_S. First, when ETVs are using the service roads G_S, they travel the shortest path on G_S, using d_S as a distance metric. We assume that they do not have to maintain distance from each other in this phase. For the aircraft, which are towed by an ETV when traversing G_X, conflicts between aircraft are avoided by imposing a minimum separation distance d_{sep} between any pair of aircraft (see Fig. 3). Aircraft are always towed to their destination using the shortest path in G_X, using d_X as a distance metric. Doing so minimizes the energy required to tow the aircraft, while separation distance infringements can be resolved by adjusting the towing speed between v_{min}^w and v_{max}^w.

2.6. ETV charging policy

Between consecutive towing tasks, ETVs may have the opportunity to recharge their batteries. This is done at one of the charging stations located along the service road, which are located at nodes $N^{CS} \subset N_S$. We use the following battery charging policy for an ETV. Firstly, partial recharging is allowed. This means that an ETV does not need to fully charge its battery during a visit to a charging station. Secondly, ETVs end their day of operations with charge Q_w (a full battery). Thirdly, the last full battery recharge is done during the night at depot $n^{dep} \in N^{CS}$. Finally, every visit to a charging station should allow at least t_{min}^c time for charging.

2.7. ETV dispatching objective

Taking into account the (i) airport layout, (ii) flight schedule for an entire day of operations, (iii) the ETV specifications, (iv) routing and charging policies, we are interesting in optimizing the ETV dispatchment such that we avoid conflicts between towed aircraft and the dispatched fleet of ETVs is optimally sized to tow all considered aircraft.
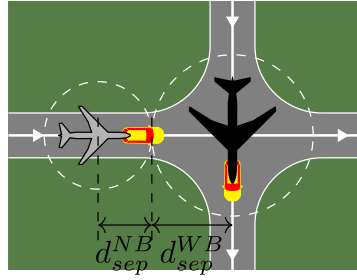
Fig. 3. Minimum distance separation between a narrow-body and a wide-body aircraft.

3. Energy consumption and charging model for ETVs

We consider the following power $P_w(v, m)$ consumed by an ETV of weight class w traveling at velocity v, with a towed mass m. If the ETV is not towing an aircraft, $m = 0$.

$$P_w(v, m) = \mu_w^g(v) \times (m_w + m) \times g \times v, \tag{1}$$

$$\mu_w^g(v) = \mu_w^0 \times \left(1 + \frac{v}{v_w^0} \right), \tag{2}$$

Here, μ^g denotes the Coefficient of Rolling Resistance, which depends on v and constants v_w^0 and μ_w^0 (Baaren and Roling, 2019).

Let q denote the total energy consumption of a towing task (aircraft towed by ETV from node n^s to n^e) or drive (ETV driving in G_S),

$$q = \int_{T'} P_w(v(t), m) \mathrm{d}t \tag{3}$$

Given that we assume a constant velocity V^s to traverse an edge in G_S and a constant velocity V^X to traverse an edge in G_X, (3) becomes:

$$q = \int_{T'} P_w(v(t), m)\mathrm{d}t = \sum_{i=1}^{k-1} \frac{d(n_i, n_{i+1})}{v_i} \cdot P_w(v_i, m), \tag{4}$$

where n_i and n_{i+1} are consecutively visited junctions in G_X or G_S, and v_i is the velocity at which the ETV travels between these nodes.

When ETVs traverse G_S, they travel the shortest path at constant velocity v_s. In this case, (4) is simplified as:

$$q_w^S(n_1, n_k) := \sum_{i=1}^{k-1} \frac{d(n_i, n_{i+1})}{v_s} \cdot P_w(v_s, m) = \frac{\sum_i d(n_i, n_{i+1})}{v_s} P_w(v_s, m) = t^S(n_1, n_k) P_w(v_s, m), \tag{5}$$

where q_w^S and t^S denote the required charge and traveling time between nodes n_1 and n_k, respectively.

ETVs can recharge their batteries at one of the charging stations. We assume that the charging time follows a bi-linear profile, used previously in Ramos Pereira (2019). Up to $\alpha Q^w (< Q^w)$, the battery is charged at a rate of P_w^c (fast-charging), and from αQ^w it becomes βP_w^c (slow-charging). Fig. 4 shows the bi-linear and actual charging profiles.

4. Linear programming formulation

The schedule management of a fleet of ETVs, i.e., deciding which aircraft is towed by which ETV and when ETVs recharge their batteries, directly depends on the way the towed aircraft are routed across the taxiway system. Firstly, the availability of an ETV for a new towing task depends on the taxi time of the previously towed aircraft. Secondly, the state-of-charge of an ETV battery depends on the energy used to tow aircraft in previous taxiing operations. The taxi time and the ETV battery state-of-charge, in turn, depend on the distance covered, and speed maintained, during taxiing.

As such, we first propose a MILP which manages the traffic of the towed aircraft on the taxiway (Section 4.1). The aircraft are routed to their destination along the shortest paths in the airport taxiway system. In order to ensure that aircraft maintain a minimum separation distance, the velocities with which they are towed are adjusted. The velocities are optimized to minimize the caused delay. The choice of routing the ETVs across the shortest path is motivated by the fact that this requires the least energy per towing, which maximizes the environmental impact of using ETVs.

Next, the obtained velocities of the towed aircraft are used to optimally schedule a fleet of ETVs (Section 4.2). We propose a second MILP to schedule ETVs either to tow aircraft or to recharge their batteries. The fleet of ETVs is sized such that all considered aircraft are towed.
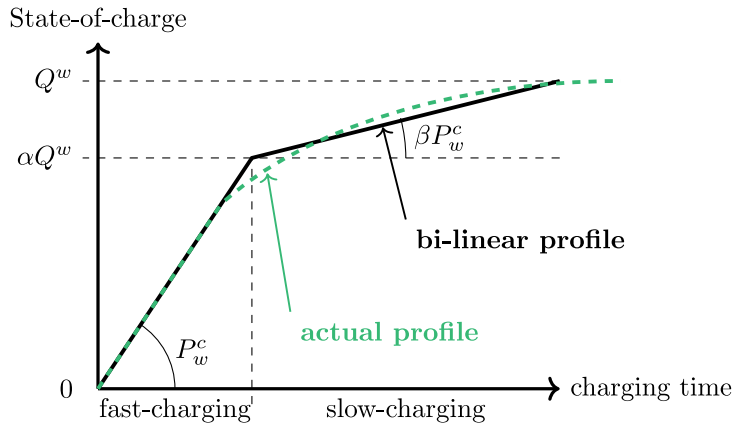
Fig. 4. The actual and bi-linear charging profile.

4.1. Phase 1 - Towing aircraft while maintaining minimum separation distance

Let us first introduce the following notation. We define a path traversed by $a \in A$ as:

Definition 4.1. The path of a towing task $a \in A$, denoted by $N_a = (n_0^a, n_1^a, n_2^a, \ldots, n_{k_a}^a)$ is the shortest path in G_X between $n^s(a) = n_0^a$ and $n^e(a) = n_{k_a}^a$, using $d_X(\cdot)$ as a distance metric. The set of all edges on the path of this aircraft is denoted as $E_a := \{(n_i^a, n_{i+1}^a)\}_{i \in \{1,\ldots,k_a-1\}}$.

For each $n \in N_X \cup N_R \cup N_G$, let $A_n \subseteq A$ be the aircraft for which $n \in N_a$. We are interested in determining the velocity at which to tow each aircraft at each road segment, i.e., the velocity profile:

Definition 4.2. A velocity profile of a towing task $a \in A^w$ is a mapping $v^a : E_a \to \mathbb{R}^+$, such that $v_{min}^w(e) \leq v^a(e) \leq v_{max}^w(e)$ for all $e \in E_a$.

For each edge $e \in E_X \cup E_X^G \cup E_X^R$ and aircraft weight class $w \in W$, the shortest and longest times in which a weight class w aircraft can traverse e are denoted as $t_{min}^w(e) = d_X(e)/v_{max}^w(e)$ and $t_{max}^w(e) = d_X(e)/v_{min}^w(e)$, respectively. The latter is always finite, and as such the aircraft never stands still during towing and the static resistance never needs to be overcome. Let $t_{min}^{end}(a) = \sum_{e \in N_a} t_{min}^w(e) + t^{Con} + \mathbb{1}_{a \in \cup_{w \in W} A^{arr,w}}(t^{PB})$ denote the earliest time at which aircraft $a \in A$ can reach its destination.

Finally, we determine the sets that describe which pairs of aircraft can cause separation distance infringements. There are three separate cases in which these infringements can occur: when two aircraft cross each other at a node, when one tries to overtake another on an edge, and when two towed aircraft encounter each other head-on on an edge. For this, let $t_{n,d}^{min}(a)$ and $t_{n,d}^{max}(a)$ denote the first and last time aircraft a can be within distance d of node n. These are determined using t_{min}^w, t_{max}^w, and $t^s(a)$.

First, let A_n^{con} denote the set of pairs of aircraft which can cause separation distance infringements at a node $n \in N_X \cup N_R \cup N_G$. Let $a, b \in A_n$ with a and b of weight classes w_a and w_b. These are included in A_n^{con} if there exists velocity profiles for a and b such that when a is at node n, b can be within the separation distance of node n or vice versa (see Fig. 3):

$$\{a, b\} \in A_n^{con} \Leftrightarrow t_{n,d}^{min}(a) \leq t_{n,0}^{max}(b) \wedge t_{n,0}^{min}(b) \leq t_{n,d}^{max}(a) \text{ with } d = d_{sep}^{w_a} + d_{sep}^{w_b}$$

Second, let A_{nm}^{ot} denote the set of pairs of aircraft which can cause separation distance infringements when towed aircraft trail each other on the same edge. Specifically, a pair of towed aircraft $a, b \in A$ with $(n, m) \in E_a \cup E_b$ is included in A_{nm}^{ot} if there exist velocity profiles for a and b such that a overtakes b on (n, m) or vice versa (see Fig. 5(a)):

$$\{a, b\} \in A_{nm}^{ot} \Leftrightarrow t_{n,0}^{min}(a) \leq t_{n,0}^{max}(b) \wedge t_{m,0}^{min}(b) \leq t_{m,0}^{max}(a)$$

Third, let A_{nm}^{ho} denote the set of pairs of aircraft which can cause separation distance infringements on a pair of edges (n, m), with $(m, n) \in E_X \cup E_X^R \cup E_X^G$, when the towed aircraft taxi in opposite directions. A pair of towed aircraft a, b such that $(n, m) \in E_a$ and $(m, n) \in E_b$ is included in A_{nm}^{ho} if there exist velocity profiles for a and b such that a is on (n, m) and b is on (m, n) simultaneously and the towed aircraft encounter each other head-on (see Fig. 5(b)):

$$\{a, b\} \in A_{mn}^{ho} \Leftrightarrow t_{n,0}^{min}(a) \leq t_{n,0}^{max}(b) \wedge t_{m,0}^{min}(b) \leq t_{m,0}^{max}(a)$$
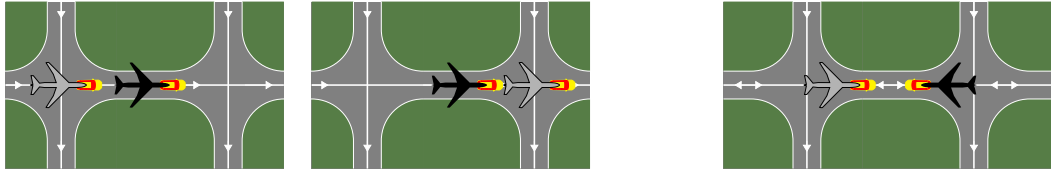
(a) Towed aircraft overtaking each other on the same taxiway. (b) Towed aircraft encountering head-on on the same taxiway.

Fig. 5. Causes for a separation distance infringement besides the situation shown in Fig. 3.

Decision variables

We consider the following set of decision variables:

$$t_n^a \in \mathbb{R}, \qquad \text{arrival time of } a \in A \text{ at } n \in N_a.$$

Using these, the velocity profile of aircraft a is given by $v^a((n,m)) = \dfrac{t_m^a - t_n^a}{d_X((n,m))}$.

We also consider the following two auxiliary decision variables to ensure a minimum separation between any two towed aircraft:

$$\Delta t_n^a \in \mathbb{R}^+, \qquad \text{time that } a \in A \text{ takes to taxi for a distance } d_{sep} \text{ after arriving at } n \in N_a,$$

$$z_n^{ab} = \begin{cases} 1, & \text{if } a \in A \text{ passes node } n \in N_a \cap N_b \text{ before } b \in A \text{ passes node } n, \\ 0, & \text{otherwise,} \end{cases}$$

such that a node $n \in N_a$ cannot be visited by other towed aircraft between t_n^a and $t_n^a + \Delta t_n^a$ without generating separation distance infringements. The values of these variables can be deduced from the t variables. If $(n,m) \in E_a$, then Δt_n^a is given by $\Delta t_n^a = (t_m^a - t_n^a)\dfrac{d_{sep}}{d_X((n,m))}$. The z variables determine the order in which the aircraft visit the nodes.

Objective function

We consider the following objective function that minimizes the maximum delay of towed aircraft as a result of keeping a minimum separation distance between any two towed aircraft:

$$\min_{t,\Delta t,z} \max_{a \in A} \left\{ t_{n^e(a)}^a - t_{min}^{end}(a) \right\}, \tag{6}$$

where $t_{n^e(a)}^a$ and $t_{min}^{end}(a)$ denote the arrival time of aircraft $a \in A$ at its destination node after ensuring a minimum separation d_{sep} with all other towed aircraft, and the earliest time at which aircraft $a \in A$ can reach its destination node, respectively.

Constraints

We consider the following constraints:

$$t_{n^s(a)}^a = t^s(a) + t^{Con} \qquad\qquad \forall w \in W, a \in A^{arr,w} \tag{7}$$

$$t_{n^s(a)}^a \geq t^s(a) + t^{Con} + t^{PB} \qquad\qquad \forall w \in W, a \in A^{dep,w} \tag{8}$$

$$t_m^a + t_{min}^w((m,n)) \leq t_n^a \qquad\qquad \forall w \in W, a \in A^w, (m,n) \in E_a \tag{9}$$

$$t_m^a + t_{max}^w((m,n)) \geq t_n^a \qquad\qquad \forall w \in W, a \in A^w, (m,n) \in E_a \tag{10}$$

$$\frac{t_n^a - t_m^a}{d_X((m,n))} - \frac{t_m^a - t_l^a}{d_X((l,m))} \leq \frac{a^{max} \times t_{min}^w((m,n))}{(v_{max}^w((l,m)))^2} \qquad\qquad \forall w \in W, a \in A^w, (l,m),(m,n) \in E_a \tag{11}$$

$$\frac{t_m^a - t_l^a}{d_X((l,m))} - \frac{t_n^a - t_m^a}{d_X((m,n))} \leq \frac{a^{max} \times t_{min}^w((m,n))}{(v_{max}^w((l,m)))^2} \qquad\qquad \forall w \in W, a \in A^w, (l,m),(m,n) \in E_a \tag{12}$$

$$\Delta t_n^a = (t_m^a - t_n^a)\frac{d_{sep}}{d_X((n,m))} \qquad\qquad \forall a \in A, (n,m) \in E_a \tag{13}$$

$$t_n^b \geq t_n^a + \Delta t_n^a - z_n^{ba}|T| \qquad\qquad \forall n \in N_X \cup N_R \cup N_G, \{a,b\} \in A_n^{con} \tag{14}$$

$$z_n^{ab} - z_m^{ab} = 0 \qquad\qquad \forall (n,m) \in E_X \cup E_X^R \cup E_X^G, \{a,b\} \in A_{nm}^{ho} \tag{15}$$

$$z_n^{ab} - z_m^{ab} = 0 \qquad\qquad \forall (n,m) \in E_X \cup E_X^R \cup E_X^G, \{a,b\} \in A_{nm}^{ot} \tag{16}$$

$$z_n^{ab} + z_n^{ba} = 1 \qquad\qquad \forall (n,m) \in E_X \cup E_X^R \cup E_X^G, \{a,b\} \in A_n^{con} \cup A_{nm}^{ho} \cup A_{nm}^{ot} \tag{17}$$

Constraint (7) ensures that all arriving aircraft start taxiing at the earliest possible moment in order to clear the runway exits as soon as possible. Constraint (8) is the equivalent of Constraint (7) for departing aircraft. In comparison to arrival aircraft, however, departing aircraft may depart later from their gate than $t^s(a)$. Constraints (9) and (10) ensure that aircraft do not taxi faster or slower

then their maximum and minimum speed, respectively. Constraints (11) and (12) limit the maximum acceleration and deceleration of the aircraft. Constraint (13) defines the time it takes an aircraft to distance itself d_{sep} from node n. Constraint (14) ensures that separation distance is maintained by any pair of towed aircraft a, b at node n, as shown in Fig. 3. Constraints (15) and (16) ensures that there are no separation distance infringements by two aircraft which use the edge in the opposite-, and the same-, direction, respectively. These correspond to Figs. 5(b) and 5(a). Finally, constraint (17) defines the order in which two aircraft a and b pass a node n.

The domain of each variable is specified in Eq. (18), (19) and (20):

$$t_n^a \in \mathbb{R} \qquad\qquad \forall a \in A, n \in N_a \qquad\qquad (18)$$

$$\Delta t_n^a \in \mathbb{R}^+ \qquad\qquad \forall a \in A, n \in N_a \qquad\qquad (19)$$

$$z_n^{ab} \in \{0, 1\} \qquad\qquad \forall n \in N_X \cup N_R \cup N_G, \{a, b\} \in A_n^{\text{con}} \qquad\qquad (20)$$

4.2. Phase 2 - Scheduling towing tasks and battery recharging moments for ETVs

Having obtained the routing of the ETVs in the taxi system, we now propose a MILP to assign ETVs to towing tasks and battery recharging moments. Since each aircraft weight class $w \in W$ has its own designated ETV type, we pose the MILP for a specific aircraft weight class.

Let $t^{end}(a) := t_{n^e(a)}^a + t^{DCon}$ denote the time an ETV finishes towing aircraft a. Let $t_{nm}^a := t_m^a - t_n^a$ denote the time a takes to traverse edge (n, m). Then, the energy needed to tow task a is given by:

$$q^X(a) := \sum_{nm \in E_a} t_{nm}^a \times P_w \left(v^a((n, m)), m(a) \right),$$

where v^a is the velocity profile of a and $m(a)$ its mass (see Section 3).

Let A_a^{in} and A_a^{out} be the set of towing tasks which can be performed before and after towing task a by the same ETV, respectively, with:

$$A_a^{in} := \{b \in A^w : t^e(b) + t^S(n^e(b), n^s(a)) \le t^s(a)\},$$
$$A_a^{out} := \{b \in A^w : a \in A_b^{in}\}.$$

In between two towing tasks a and b, ETVs may have the opportunity to recharge their battery at a charging station in N^C. ETVs always use the charging station closest to their next towing task. We denote this station by $n^C(b)$. For simplicity, we introduce the following abbreviations for the required energy of several types of movements of ETVs on the service road system (see Section 3):

$$q_f^S(a) := q_w^S(n^{dep}, n^s(a)),$$
$$q_l^S(a) := q_w^S(n^e(a), n^{dep}),$$
$$q^S(a, b) := q_w^S(n^e(a), n^s(b)),$$
$$q_C^S(a, b) := q_w^S(n^e(a), n^{CS}(b)) + q_w^S(n^{CS}(b), n^s(b)),$$
$$q_C^S(a) := q_w^S(n^{CS}(a), n^{st}(a)).$$

Here, q_f^S denotes the energy required to drive from the ETV depot to the start of a task, and q_l^S denotes the energy required to drive from the end of a task to the depot. These are the first and last movements made by an ETV on the day of operations. Also, $q^S(a, b)$ and $q_C^S(a, b)$ denote the energy to drive directly from the end of task a to the start of task b directly and via charging station $n^C(b)$, respectively. Finally, $q_C^S(a)$ denotes the energy required to drive from the charging station $n^C(a)$ to the start of task a.

For a pair of towing tasks a and b, let $t^c(a, b)$ denote the available time for charging between these tasks:

$$t^c(b, a) := \left[t^s(a) - t^S(n^{CS}(a), n^s(a)) \right] - \left[t^e(b) + t^S\left(n^e(b), n^{CS}(a) \right) \right]$$

Finally, between performing two towing tasks a and b, an ETV is allowed to recharge if two conditions are met: (i) the ETV should be able to arrive at b with a higher state of charge after recharging than if it drives directly from a to b, (ii) the available charging time is at least t_{min}^c. For a towing task a, let $A_{C,a}$ denote the set of tasks which can be executed before task a for which these two conditions hold,

$$A_{C,a} := \{b \in A_a^{in} : t^c(b, a) > t_{min}^c \wedge q^{dr}(b, a) > q_{CS}^{dr}(b, a) - t^c(b, a) \cdot P_w^c\}.$$

Decision variables

We consider the following decision variables, which determine the order in which the towing tasks are performed by the ETVs:

$$x_{ab} = \begin{cases} 1 & \text{if aircraft } a \text{ is towed directly before } b, \\ 0 & \text{else}, \end{cases}$$

$$x_a^f = \begin{cases} 1 & \text{if aircraft } a \text{ is the first the ETV tows in a day}, \\ 0 & \text{else}, \end{cases}$$

$$x_a^l = \begin{cases} 1 & \text{if aircraft } a \text{ is the last the ETV tows in a day,} \\ 0 & \text{else.} \end{cases}$$

Additionally, the q variables keep track of the state-of-charge of the ETV batteries:

$q_a \in \mathbb{R}$ ETV battery charge at start of task a.

Objective function

We consider the following objective function that minimizes the number of ETVs required to perform all towing tasks during a day:

$$\min_{x,q} \sum_{a \in A^w} x_a^f \tag{21}$$

Constraints

We consider the following constraints:

$$x_a^f + \sum_{b \in A_a^{in}} x_{ba} = 1 \qquad \forall a \in A^w \tag{22}$$

$$x_a^l + \sum_{b \in A_a^{out}} x_{ab} = 1 \qquad \forall a \in A^w \tag{23}$$

$$q_a \le Q_w - x_a^f q_f^S(a) + Q_w(1 - x_a^f) \qquad \forall a \in A^w \tag{24}$$

$$0 \le q_a - x_a^l(q^X(a) + q_l^S(a)) + Q_w(1 - x_a^l) \qquad \forall a \in A^w \tag{25}$$

$$q_b \le q_a - x_{ab}(q^X(a) + q^S(a,b)) + Q_w(1 - x_{ab}) \qquad \forall b \in A^w, a \in A_b^{in} \setminus A_{C,b} \tag{26}$$

$$q_b \le q_a - x_{ab}(q^X(a) + q_C^S(a,b) - P_w^c \cdot t^c(a,b)) + Q_w(1 - x_{ab}) \qquad \forall b \in A^w, a \in A_{C,b} \tag{27}$$

$$q_b \le q_a - x_{ab}(q^X(a) + q_C^S(a,b)) + Q_w(1 - x_{ab}) + $$
$$(1 - \beta)(\alpha Q - (q_a - x_{ab}(q^X(a) + q_C^S(a,b)))) + \beta P_w^c t^c(a,b) \qquad \forall b \in A^w, a \in A_{C,b} \tag{28}$$

Eqs. (22) and (23) ensure that each towing task is executed by exactly one ETV. Eq. (24) limits the state-of-charge of the ETV whent a is the first task performed by that ETV in a day. Eq. (25) ensures after an ETV performs its last task in a day, then that ETV still has enough energy to reach the depot. Eq. (26) limits the battery charge between tasks if the ETV does not visit a charging station in-between these tasks. Eqs. (27) and (28) calculate the new state of charge if a charging station is visited and fast or slow charging is used, respectively (see Fig. 4). Finally, the domain of each decision variable is specified in Eqs. (29) and (30):

$$x_{ab}, x_a^f, x_a^l \in \{0, 1\} \qquad \forall a \in A, b \in A_a^{out} \tag{29}$$

$$q^X(a) \le q_a \le Q_w - q_C^S(a) \qquad \forall a \in A. \tag{30}$$

5. Case study: Dispatching a fleet of ETVs at Amsterdam Airport Schiphol

Airport taxi system and service road system

Fig. 6 shows the runway entrances and exists, N^R, and the gate nodes, N^G, together with the connecting road networks at AAS (based on the Schiphol aerodrome charts LVNL - Air Traffic Control the Netherlands, 2019). In total, there are 6 runways and 7 piers (B, C, D, E, F, G, H/M). These are converted to 10 runway nodes and 9 gate nodes, indicated by vertically hatched circles on the map. The edges of the taxiway and service road networks, which connects N^G and N^R, are indicated with solid and dashed lines, respectively. In the taxiway network, some of the edges can be traversed in one direction only, and this is indicated by arrows. We assume five charging stations $N^{CS} = \{C1, C2, C3, C4, C5\}$ are available at AAS (indicated with horizontally hatched circles in Fig. 6). We also assume that the ETV depot is centrally located at station $n^{dep} = C5$.

Aircraft to be towed at AAS during one day of operations

We consider the flight schedule of an entire day of operations at AAS, with data from the day of operations of December 14, 2019. Fig. 7 shows the distribution of the earliest time to start towing, t^s, for all flights considered. This schedule consists of 913 flights (750 narrow-body, 147 wide-body, and 16 heavy-wide-body aircraft), arriving and departing on this day of operation. In 2019, the average number of arriving and departing flights at AAS was 1230 (Schiphol, 2019b), making the 14th of December 2019 a relatively quiet but still representative day of traffic at AAS. Additionally, this selected day exhibits a varied mix of runway configurations since five out of the six runways at AAS (18R-36L, 18L-36R, 09-27, 04-22, and 06-24) are being used in eight different runway configurations throughout the day.

ETV specifications

Table 1 shows the ETV specifications assumed for our case study. These specifications are a function of the aircraft weight class (Table 1a) as well as additional non-weight-related parameters (Table 1b).
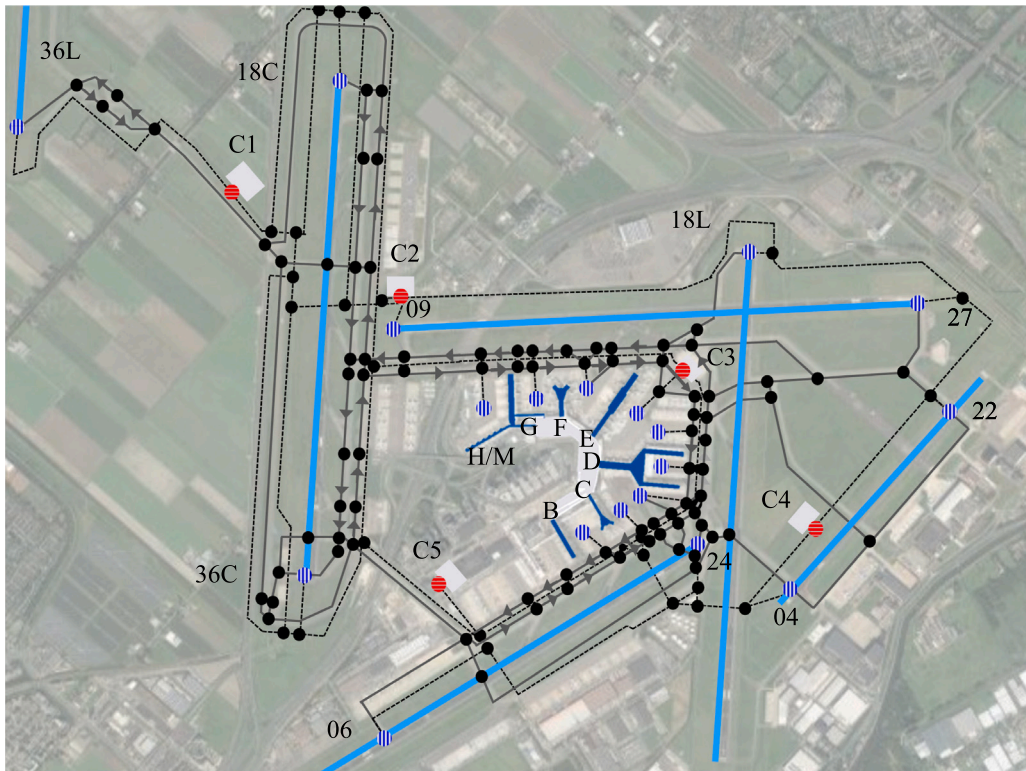
Fig. 6. Runways N^R and gate nodes N^G, together with taxiways (solid lines), service roads (dashed lines) and charging stations (C1, ..., C5) at AAS. The map is based on the Schiphol aerodrome charts (LVNL - Air Traffic Control the Netherlands, 2019).
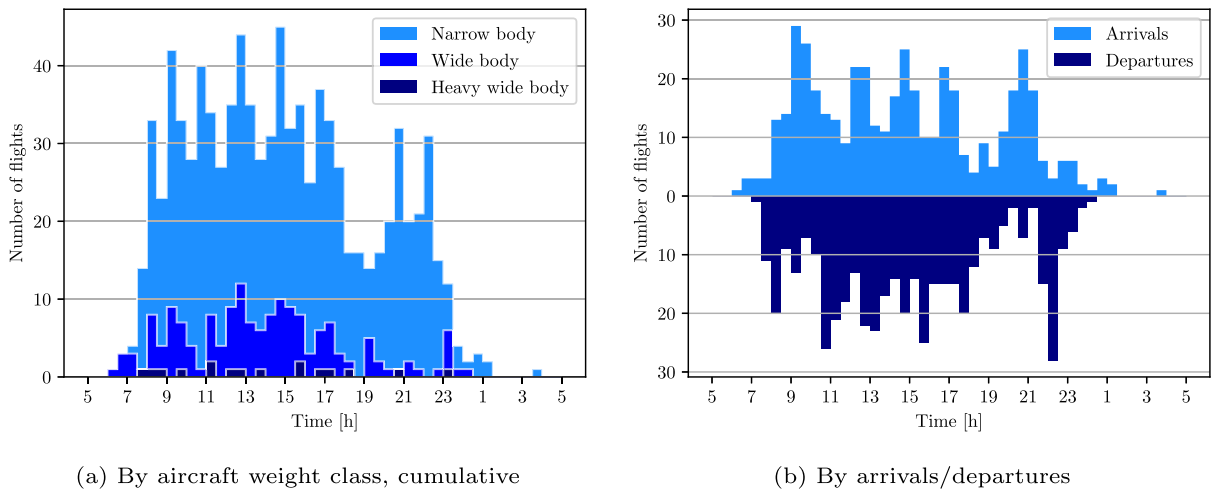

(a) By aircraft weight class, cumulative

(b) By arrivals/departures

Fig. 7. Distribution of the earliest time to start towing, t^s, for all flights arriving/departing at AAS on December 14, 2019.

5.1. Results - Dispatching a fleet of ETVs at AAS

Results Phase 1 - Taxiing towed aircraft while avoiding separation distance infringements

Fig. 8 shows the results obtained for the Phase 1 MILP. Fig. 8(a) shows a histogram of the additional taxi time needed for ETVs to keep a minimum separation distance d_{sep}, i.e., $t^a_{n^e(a)} - t^{end}_{min}(a)$ for all $a \in A$. The maximum obtained additional taxi time is 90 s. Of the total 913 aircraft, only 26 aircraft require an additional taxi time of more than 60 s.
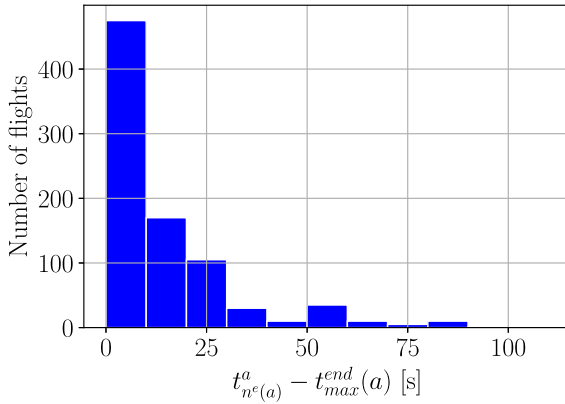
Fig. 8(b) shows the average additional taxi time required by ETVs per 30 min time windows. The highest additional taxi times are required during the peak hours of 11 AM, 1 PM and 3 PM. During these time periods, the number of arrivals at the airport is

Table 1
Electric towing specifications.

(a) Parameters dependent on the aircraft weight class.

	Explanation	Value			Ref
w	Weight class	NB	WB	H-WB	
v_w [km/h]	Maximum towing speed	42.5	37	37	Lukic et al. (2019)
P_w^c [kW]	Charging power	100	350	500	Baaren and Roling (2019)
m_w [10^3 kg]	ETV mass	15	35	50	Baaren and Roling (2019)
Q_w [kWh]	Battery capacity	400	1250	3200	Baaren and Roling (2019)
d_{sep}^w [m]	Separation distance	40	50	60	

(b) Additional parameters.

	Explanation	Value
t_{min}^c [h]	Minimum charging time	1
t^{ECD} [s]	Engine-cool-down-time	180 (Dzikus et al., 2013)
t^{Con} [s]	Connect-time	60
t^{PB} [s]	Push-back-time	120 (Dieke-Meier and Fricke, 2012)
t^{DCon} [s]	Disconnect-time	60 (Dieke-Meier and Fricke, 2012)
t^{EWU} [s]	Engine-warm-up-time	300 (Dzikus et al., 2013)
α	Charging curve coefficient	0.9 (Ramos Pereira, 2019)
β	Charging curve coefficient	0.1 (Ramos Pereira, 2019)
μ_0	Rolling resistance coefficient	0.1 (Daidzic, 2017)
v_0 [km/h]	Rolling resistance base velocity	41.16 (Daidzic, 2017)
v_s [km/h]	Service road velocity	30 (Health, Safety and Environment office Schiphol, 2020)

(a) Histogram of the additional taxi time.
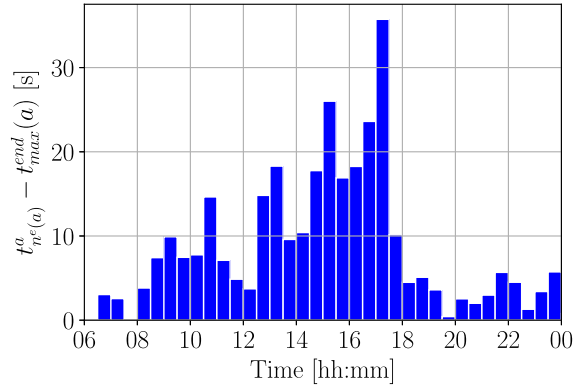
(b) Average additional taxi time every half-hour.

Fig. 8. Distribution of the additional required taxi time, $t_{n^e(a)}^a - t_{min}^{end}(a)$, in order to avoid separation distance infringements.

similar to the number of departures, as can be seen in Fig. 7(b). This causes large streams of in-and-outbound aircraft to be towed in opposite directions on some of the bidirectional roads in the taxiway network, which may lead to head-on encounters. Solving for these potential head-on separation distance infringements leads to longer taxiing times, compared to solving for infringements caused by trailing aircraft.

Fig. 9 shows an example of a resolved minimum separation infringement between arriving and departing aircraft in the period 11:15–11:16 AM. The movements of aircraft 112, 114 and 115 are considered during these 60 s Departing narrow-body aircraft 112 (Embraer 190) is towed by an ETV from pier E to runway entrance 24. It is trailed by narrow-body aircraft 114 (Embraer 175), which is also headed for runway entrance 24, but from pier D. These two aircraft meet arriving wide-body aircraft 115 (Boeing 787), which is towed from runway exit 04 to pier C. Should these aircraft use the fastest velocity profile on the shortest path from their origin node to destination node, then aircraft 112 and 115 intersect head-on in the taxi system between 11:15:20 and 11:15:40. Also, aircraft 114 will be within the minimum separation distance of aircraft 115 at 11:15:40. To avoid these two separation infringements, Model 1 specifies velocity profiles such that aircraft 112 and 114 are slowed down in order to let aircraft 115 pass before them.

Results Phase 2 - Scheduling towing tasks and battery recharging moments for ETVs

Fig. 10 shows the ETVs' schedule for aircraft towing and recharging times when given the flight schedule of December 14, 2019 at AAS. A total of 38 ETVs are required to tow the aircraft. Out of these 38 ETVs, 26 ETVs are required for narrow-body aircraft, 10 ETVs are required for wide-body aircraft and 2 ETVs for heavy wide-body aircraft. At any moment in time, an ETV is either:
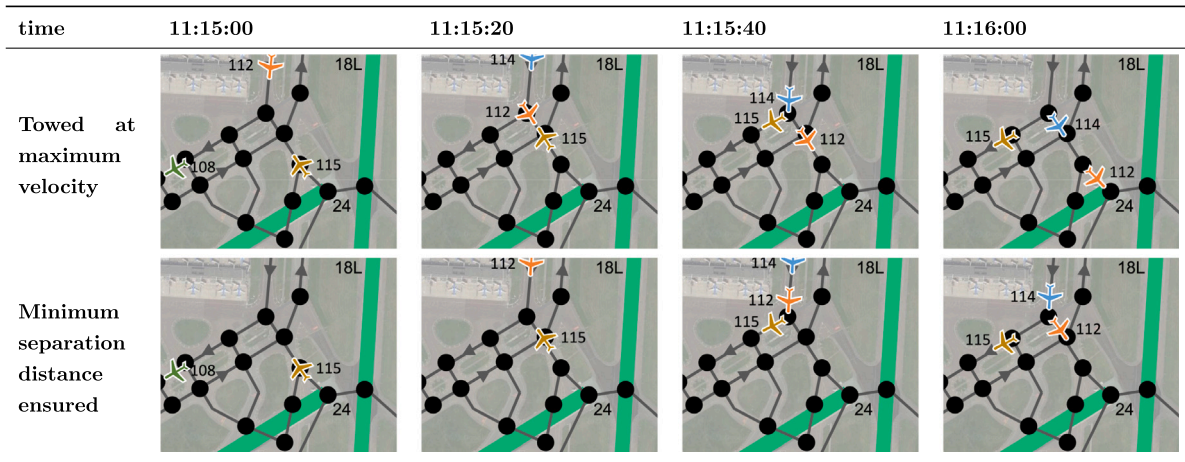
time	11:15:00	11:15:20	11:15:40	11:16:00
Towed at maximum velocity				
Minimum separation distance ensured				

Fig. 9. Example — unrestricted aircraft velocity profile vs. the velocity profile proposed by Model 1, aircraft 112, 114, 115.

Table 2
Average utilization time of the ETVs from each weight class, for the three activities: towing, driving, and charging.

w	Driving [hh:mm]	Towing [hh:mm]	Charging [hh:mm]	Total [hh:mm]
NB	04:15	04:34	09:16	18:05
WB	02:21	02:21	03:54	8:47
H-WB	01:14	01:13	03:12	5:39

(i) towing an aircraft in the taxi system G_X (towing), (ii) traversing the road system G_S (driving), (iii) recharging its battery at a charging station (charging), or (iv) waiting at a gate node, a runway exit or charging station (idle). When a ETV is in which state is indicated in Fig. 10.

For heavy-wide body aircraft, two ETVs are needed since there are two simultaneous towing tasks around 4 PM. For wide-body aircraft, around 12 PM, there are 10 simultaneous towing tasks which leads to a need for 10 wide-body ETVs. These two moments are indicated by vertical lines in Fig. 10. The number of narrow-body ETVs, however, is not limited by the number of simultaneous towing tasks. In fact, there are never 26 simultaneous towing tasks for narrow-body aircraft. The number of narrow-body ETVs is constrained by the battery specifications (limiting battery capacity and charging power).

The fact that the number of ETVs for narrow-body aircraft is limited by the battery specification is corroborated by Fig. 11, which shows the state-of-charge for each of the ETVs throughout the day. The difference between fast- and slow-charging can be seen in this figure. The results show that the narrow-body ETV schedule is so tight that it requires the full charge of the ETVs to be used. In contrast, the wide-body and heavy-wide-body ETVs require only 85% to 50% of their battery capacity, respectively, to carry out the schedule.

Table 2 shows the average time an ETV is either driving in the service road system G_S, towing an aircraft in the taxi system G_X, or charging its battery at a charging station. The ETVs spend similar fractions of their time towing, driving, or charging their batteries. As expected, ETVs for narrow body aircraft are utilized the highest fraction of the time, since the narrow body flight schedule is also comprised of the most flights and the most even distribution of flights throughout the day.

5.2. Computation time vs. Number of towing tasks

Table 3 shows the total computational time required to obtain an optimized ETV fleet dispatchment for a day of operations for various flight schedule sizes. These results have been obtained with the Gurobi Optimizer 9.1, using an Intel Core i7-10610U. Here, the flight arrival and departure times are distributed throughout the day according to the distributions given in Fig. 7. For a flight schedule with 2000 flights on a single day, corresponding to the number of flights at the worlds busiest airports (Berthier, 2021), the ETV dispatchment is obtained in 7366 s, out of which 5745 s are needed to determine the ETV velocity profiles (Model 1), and 1621 s to create the ETV towing and battery charging schedule (Model 2).

5.3. Electric aircraft towing during various levels of congestion at AAS

In order to evaluate our model for various levels of congestion at AAS, we apply our two-phase scheduling algorithm for additions days of operation. We consider four additional flight schedules from 2019 which range from ordinary to relatively busy days: March 9 (866 flights), April 13 (1080 flights), May 11 (1191 flights), and June 15 (1278 flights). Fig. 12 shows the distribution of t_s of the arriving and departing flights on these days.
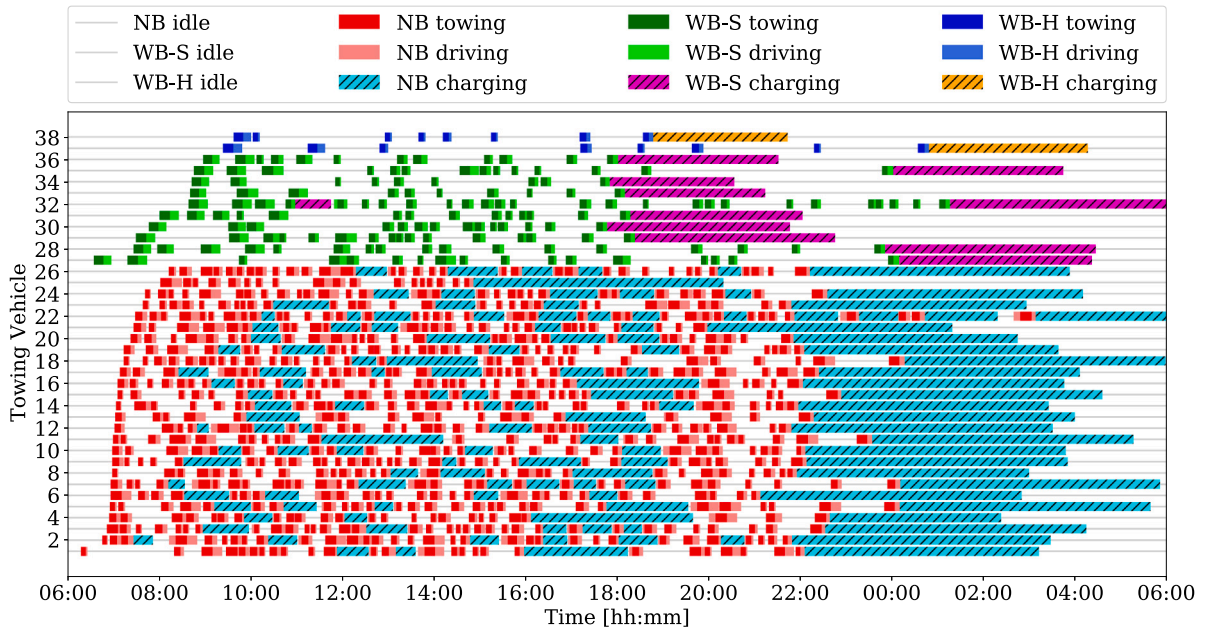
Fig. 10. ETV schedule for aircraft towing and battery recharging — December 14, 2019.
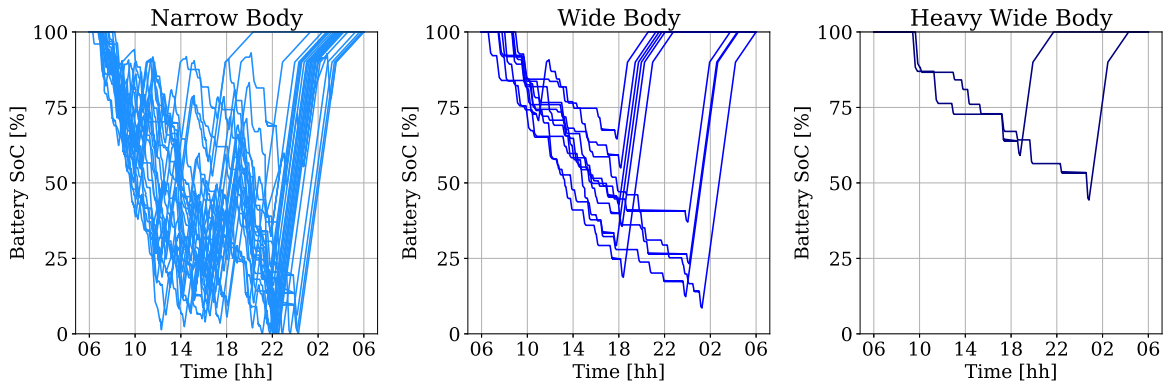

Fig. 11. State-of-charge of all dispatched ETVs, sorted by weight class, during the day of operations.

Table 3
Running time of the Phase 1 and Phase 2 MILPs for different flight schedule sizes.

Number of towing tasks	100	200	500	1000	1500	2000
Phase 1 [s]	9.42	22.3	118.1	498.3	1832	6442
Phase 2 [s]	0.19	0.91	9.54	79.2	580.3	1712
Total [s]	9.61	23.2	127.6	577.5	2412	8158

The minimum required number of ETVs to tow all flights on these days is given in Table 4. The ETV fleet size ranges from 39 (on March 9) to 50 (on June 15). It is interesting to note that while there are fewer flights on March 9 than there are on December 14, the required ETV fleet is larger. This can be explained by the relatively busy peak hours on March 9 (see Fig. 12).

Fig. 13 shows the average number of flights towed by an ETV for each weight class per day. The high narrow-body ETV utilization, which increases for increasingly large flight schedules, stands out. This is the results of the greater abundance of flights to which an ETV can be assigned; the same reason that narrow-body ETV utilization is relatively high compared to (heavy-)wide-body ETV
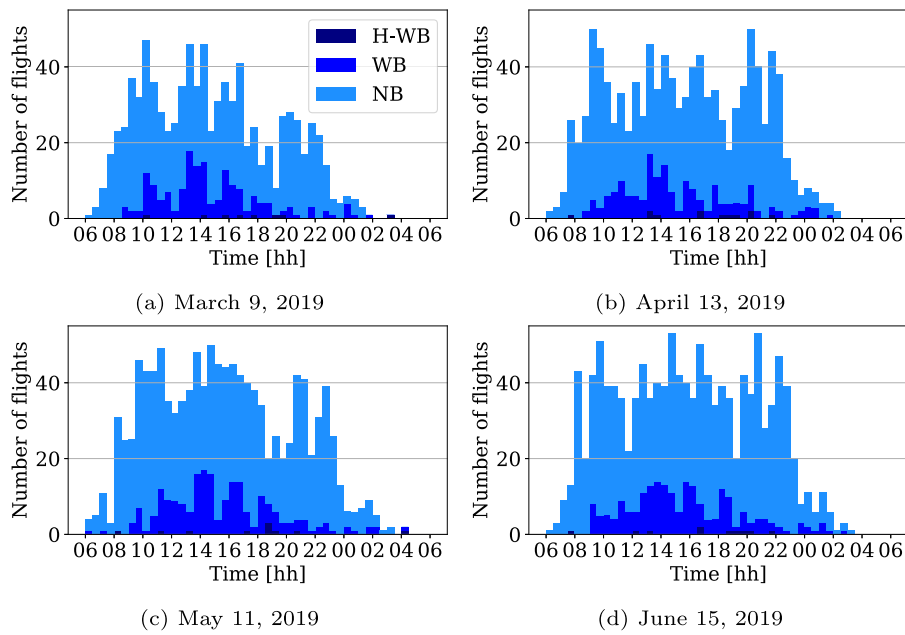
(a) March 9, 2019   (b) April 13, 2019

(c) May 11, 2019   (d) June 15, 2019

Fig. 12. Distribution of t^s for four different days during 2019 at Amsterdam Airport Schiphol, per weight class.

Table 4
Number of required ETVs for different flight days.

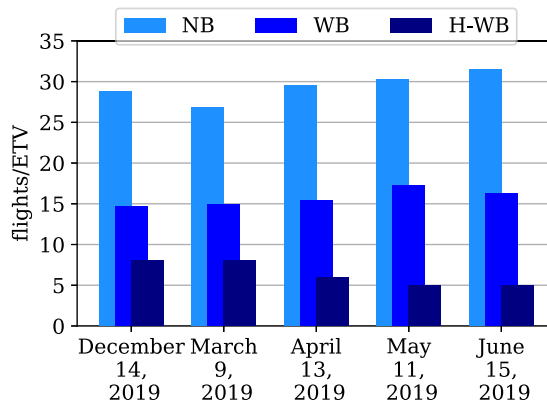| Day		NB	WB	H-WB	Total
December 14,	FL	750	147	16	913
2019	ETV	26	10	2	38
March 9,	FL	724	164	8	896
2019	ETV	27	11	1	39
April 13,	FL	914	154	12	1080
2019	ETV	35	10	2	47
May 11,	FL	969	190	10	1191
2019	ETV	36	11	2	49
June 15,	FL	1040	195	10	1258
2019	ETV	37	12	2	50

Fig. 13. Number of flights per ETV for the different days in 2019.

utilization. Finally, for large flight schedules, it can be observed that the number of flights per ETV is approximately constant for each weight class, and hence that the number of ETVs grows approximately linearly with the number of flights.

6. The Greedy ETV Fleet Dispatching algorithm

In this section, we propose a Greedy ETV Fleet Dispatching algorithm (GEFD), which can easily be implemented in practice, and has a very competitive computational time. We are interested in assessing the performance of the GEFD algorithm against our proposed optimal ETV dispatching model (see Section 4).

6.1. The greedy ETV fleet dispatching (GEFD) algorithm

Similar to Section 4, the GEFD performs three tasks: it routes the aircraft across the taxiway system G_X, assigns the aircraft to ETVs, and determines when the ETVs recharge their batteries. Compared with the optimization model in Section 4, the GEFD algorithm processes towing tasks sequentially rather than simultaneously.

Let E be a set of ETVs. We define the state of an ETV as follows:

Definition 6.1. An ETV $e \in E$ is said to be in state $S_e \in S$, $S = (N^R \cup N^G \cup N_X \cup N_S) \times T \times \mathbb{R}^+$, where $S_e = (l_e, t_e, q_e)$ gives the position, time, and state-of-charge of the battery of ETV e at a specific moment, respectively.

Whether an ETV is able to tow an aircraft depends on the last known state of this ETV since it needs to be able to reach the aircraft in time, and it has to have sufficient battery charge.

Definition 6.2. Let the function $C : S \times A \rightarrow \mathbb{R}$ denote the highest state of charge with which an ETV e can reach towing task $a \in A$, given its state S_e. It is the maximum of the two following states-of-charge:

  (i) The state-of-charge of e when it drives directly from S_e to $n^s(a)$,
  (ii) The state-of-charge of e when it drives to $n^s(a)$ via a charging station and charges its battery for as long as possible, while still arriving before $t^s(a)$.

Finally we determine which ETVs are able to tow a towing task, given their last fixed states:

Definition 6.3. Given its state S_e, an ETV e is able to perform towing task $a \in A$ if:

  (i) it is of the same weight class as the to-be-towed aircraft,
  (ii) it is able to arrive at a before $t^s(a)$,
  (iii) $C(S_e, a)$ is large enough for e to tow a, reach a charging station and fully recharge its battery before the end of the day.

The GEFD algorithm attempts to maximize the utilization of each ETV by sequentially assigning those ETVs to towing tasks that have the highest state-of-charge. This contributes to a fair workload distribution between the ETVs and a maximization of the number of aircraft an ETV tows per day. Battery charging is done opportunistically: if an ETV is idle for longer then t^c_{min} in-between two consecutive towing tasks, then this ETV will recharge its battery.

The algorithm is initialized for an ETV fleet size of 0 (line 1) and iterates over the fleet sizes using a bisection algorithm up to $|A^w|$. During every iteration, an ETV fleet is initialized where all vehicles are located at the depot at the start of the day with full batteries (line 5). To allocate all vehicles, the algorithm loops over the towing tasks (line 7) in ascending order of t_s. Each step it (i) determines the set L of ETVs which are able to tow task a (line 11, using Definition 6.3), and (ii) allocates the ETV $\hat{e}$ to a which can start towing it with the highest state of charge (line 18). The towing task is routed to its destination across the shortest path, while ensuring that the minimum separation distance is maintained from all previous towed aircraft using a time dependent shortest path algorithm (line 19, see e.g. Chon et al., 2003). The state of $\hat{e}$ is updated to its state at the moment when it has just detached from a (line 20). If there are no ETVs available to tow a, the fleet size is increased using the bisection algorithm (line 14), and the fleet is reassigned from the start of the day to ensure a fair workload distribution. If this does not occur, the fleet size is decreased using the bisection algorithm. Once the optimal fleet size is found, the GEFD algorithm terminates.

6.2. Results - the GEFD algorithm

We apply the GEFD algorithm at AAS using the same flight schedule as before of December 14, 2019. We have previously used this flight schedule to determine the performance of the models in Section 5.

First, we compare the results of the Phase 1 MILP from Section 4 and the aircraft routing of the GEFD algorithm. Fig. 14 shows the additional required taxi time to avoid separation distance infringements obtained with both the GEFD algorithm and the Phase 1 MILP. Fig. 14(a) shows the distribution of the additional required taxiing time for both algorithms. The results show that using the GEFD algorithm gives higher additional taxi times for towed aircraft, up to a maximum of 110 s. The average additional taxi times of the Phase 1 MILP and the GEFD algorithm are 10.2 s and 13.4 s, respectively, resulting in an optimality gap of 22% when compared to the MILP model.

Fig. 14(b) shows the distribution of the average additional taxi time throughout the day of operations. Specifically, the difference in the average additional taxi times between the Phase 1 MILP and the GEFD algorithm is shown. The results show that the largest differences can be found at the end of the peak hours: during 9:00–10:00 after the morning peak, during 14:00–15:00 after the

---

Algorithm 1: The GEFD (Greedy ETV Fleet Dispatching) algorithm

Data: Airport layout, Flight schedule A, ETV specifications
Result: ETV fleet size n_w for all weight classes, assignment of ETVs to aircraft, schedule of ETV recharge times

1 Initialize $n_w = 0$ for all $w \in W$;
2 Sort A by increasing t^s values;
3 **while** $n_w \leq |A^w|$ *for all* $w \in W$ **do**
4   **for** $w \in W$ **do**
5   Initialize fleet E of size n_w, all ETVs have state $S_e = (t_e = 0, l_e = n^{dep}, q_e = Q_w)$;
6   **end**
7   **for** $a \in A$ **do**
8   **for** $e \in E$ **do**
9   Determine $C(S_e, a)$;
10   **end**
11   Determine the ETVs which can tow a, denote this set as $L \subset E$;
12   **if** $L = \emptyset$ **then**
13   Let w be the weight class of a;
14   Increase n_w according to bisection algorithm ;
15   Go to line 3;
16   **else**
17              $\hat{e} = \text{argmax}_{e \in L} C(S_e, a)$;
18   Assign a to $\hat{e}$;
19   Route a across the taxiway system using $\hat{e}$;
20              $S_e \leftarrow (n^e(a), t^e(a), C(S_{\hat{e}}, a) - q^X(a))$;
21   **end**
22   **end**
23   Send all $e \in E$ to n^{dep} and charge;
24   Decrease n_w according to bisection algorithm;
25 **end**
26 **if** $\exists w \in W : n_w > |A^w|$ **then**
27   Instance is infeasible;
28 **else**
29   Solution found, terminate algorithm;
30 **end**
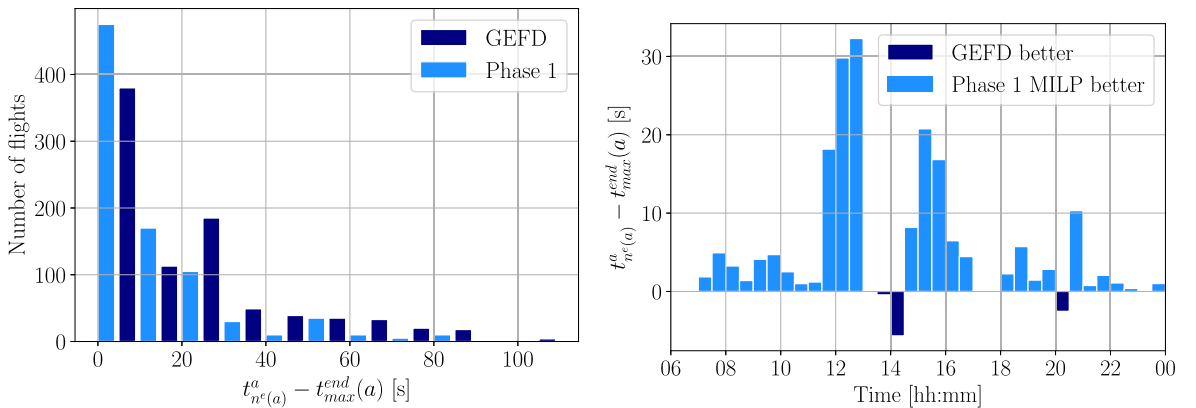
(a) Histogram of the additional taxi time for the optimization and the GEFD algorithm.

(b) Difference in the average additional taxi time every half-hour between the optimization and the GEFD algorithm.

Fig. 14. Distribution of the additional required taxi time, $t^a_{n^e(a)} - t^{end}_{min}(a)$, in order to avoid separation distance infringements.

first afternoon peak, and during 15:30–16:00 after the second afternoon peak. This reflects the characteristic of the GEFD algorithm which processes aircraft sequentially, instead of simultaneously, and thus postpones adding additional taxi times to AC it processes later.

Table 5
Average utilization time of the ETVs from each weight class, for the three activities: towing, driving, and charging.

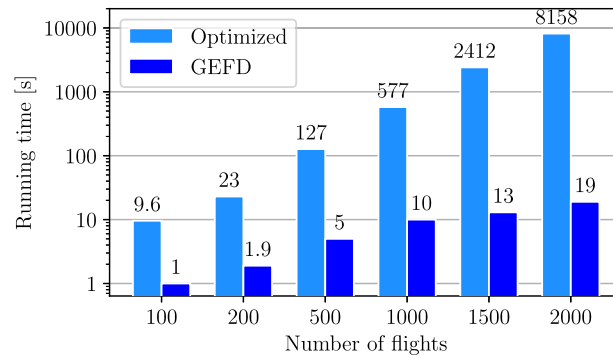| w	Driving [hh:mm]	Towing [hh:mm]	Charging [hh:mm]	Total [hh:mm]
NB	04:10	04:05	08:32	16:47
WB	02:08	02:19	04:02	8:29
H-WB	01:14	01:13	03:09	5:36

Fig. 15. Running time of optimization models and the GEFD algorithm — various flight schedule sizes.

Comparing the Phase 2 MILP and the GEFD algorithm, the results indicate that the GEFD algorithm requires an ETV fleet of 28 narrow-body, 10 wide-body, and 2 heavy-wide-body ETVs. This is only two more ETVs for the first weight class (see Fig. 10).

Table 5 shows the utilization of the different ETVs for the solution obtained with the GEFD algorithm. The heavy-wide-body utilization is the same as when using our optimization model (see Table 2). For the wide-body class, the average towing time is the same in the case of our optimization model, while the driving and charging times are smaller. This is due to the fact that the GEFD scheduled for towing the ETV which can have the highest state of charge. When considering the difference in fleet size (26 against 28) the same can be found for the narrow-body weight class.

6.3. Sensitivity to the number of towing tasks

In this section we compare the performances of the GEFD algorithm with the MILP ETV dispatchment optimization models on flight schedules of different sizes. These are the same ones as used in Section 5.2.

We first consider the computational efficiency of both methods. Fig. 15 shows the running time of the GEFD algorithm against our optimization models. For 100 towing tasks, the GEFD requires 1.04 s against 9.61 s for the optimal model. For 2000 towing tasks, the running time of the GEFD algorithm is more then a hundred times faster then our optimization model, requiring 19 s against 8158 s.

Next, we consider the objective value attained by both methods. Fig. 16(a) shows the required number of ETVs for both the optimization and the GEFD algorithm for different sizes of the flight schedule. The results show that, to be able to tow all considered aircraft, the GEFD algorithm requires the same fleet size up to 200 towing tasks. However, for the instances with 500 or more towing tasks, the GEFD algorithm requires 2 through 4 additional ETVs to be able to tow all considered aircraft. However, the impact that this increase of the fleet of up to 6% has is relatively limited, as we shall show in the with the next result.

Finally, we study the impact of the difference between the fleet sizes of the GEFD algorithm and our optimization models. In Fig. 16(b), the GEFD algorithm is used but constrained to the fixed ETV fleet size determined using our Optimization algorithm as graphed in Fig. 16(a). Specifically, the GEFD algorithm dispatches 11, 16, 31, 56, 74, and 92 ETVs to the flight schedules with 100, 200, 500, 1000, 1500, and 2000 towing tasks, respectively. When this fleet size is smaller then the one originally generated by the GEFD algorithm, also shown in Fig. 16(a), not all aircraft can be towed because of scheduling conflicts. These aircraft have to taxi on their own, and the number of times this occurs is graphed in Fig. 16(b).

Only in the case of a flight schedule with 100–200 arriving and departing aircraft, the ETV fleet size determined using our optimization model is sufficiently large to tow all considered aircraft using the GEFD algorithm. For larger flight schedules, several aircraft cannot be towed by ETVs. For example, when considering 500 arriving and departing aircraft, there are not sufficiently many ETV to tow 2 of these. When considering 2000 arriving/departing aircraft 12 of these are not towed due to lack of available ETVs.

6.4. Rolling horizon scheduling when considering flight delays

As discussed in the previous subsection, the major advantage of the GEFD algorithm is that it has a relatively low running time. This presents the opportunity to reevaluate the ETV schedule in real-time when flight delays occur. In this section, the ability to dynamically schedule ETVs of the GEFD algorithm is compared with the MILP ETV dispatchment optimization algorithm.
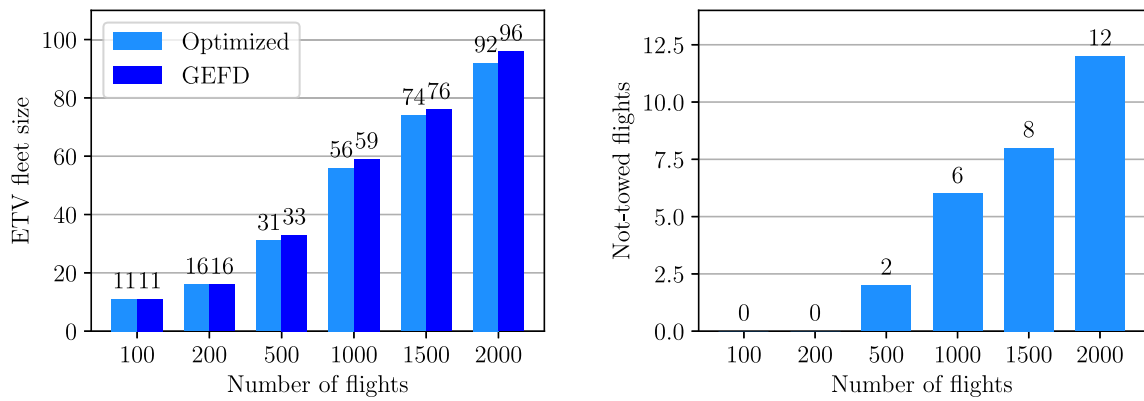
(a) Required ETV fleet size to be able to tow all flights when using the optimization and GEFD algorithms.

(b) Number of not towed flights when applying GEFD to to optimal fleet size. Non-zero when the GEFD required extra ETVs.

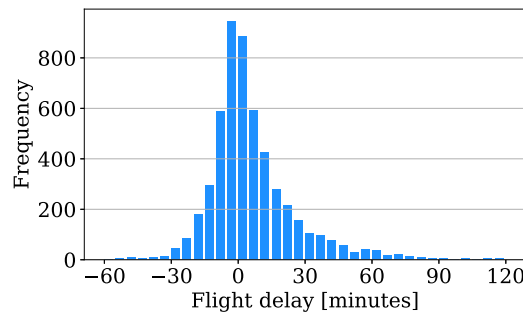**Fig. 16.** Performance of the optimization model (Section 4) vs. the GEFD algorithm.

Fig. 17. Distribution of flight delays on March 9, April 13, May 11, June 15, and December 14, 2019 at AAS.

Table 6

Flights not towed by ETVs when using the rolling horizon approach with the MILP ETV fleet dispatchment optimization and the GEFD heuristic algorithm. The not-towed flights are given in absolute numbers (#) and as a percentage of the total number of flights (%).

Day of operation (2019)			Dec 14	Mar 9	Apr 6	May 7	Jun 15	Total
Number of flights			913	896	1080	1191	1258	5338
Not-towed flights	MILP	#	8	4	14	21	27	74
		%	0.9	0.6	1.3	1.6	2.1	**1.4**
	GEFD	#	26	29	42	57	75	229
		%	2.8	3.2	3.9	4.7	6.0	**4.3**

The problem is now considered from a rolling horizon perspective: twice every hour the flight schedule is updated and the ETV schedule may be reevaluated. We assume that the flight delay is known thirty minutes before the actual arrival/departure time. Throughout the day no ETVs may be added to the schedule, and the new objective is to tow as many flights as possible. Both the GEFD and the MILP formulation are relaxed in order to allow flights to taxi without an ETV.

The rolling horizon approach is applied to the flight schedules from March 9, April 13, May 11, June 15, and December 14 of 2019. Fig. 17 shows the flight delays on these days; they have an average delay of 8 min with a standard deviation of 19 min. The minimum required fleet size for each day of operations, From Table 4, has been used.

Fig. 18 illustrates how the schedule of one narrow-body ETV evolves during the day of operation, in snapshots every three hours. The vertical red dashed lines show the current time. The distinction is made between already performed and planned events (tows, drives and charges).

Table 6 shows the number of flights which have not been towed after applying the rolling horizon approach for both methods. The not-towed flights are given both in absolute numbers and as a percentage of the total number of flights. The results show that there is a performance gap between the MILP and the GEFD, as they require 1.4% and 4.3% of the flights to taxi without ETV, respectively. Second, the algorithms assign a smaller fraction of flights to ETVs when the flight schedule becomes larger. This illustrates that increasing the utilization time of the ETVs (Fig. 13) reduces the robustness of the schedule to delays.
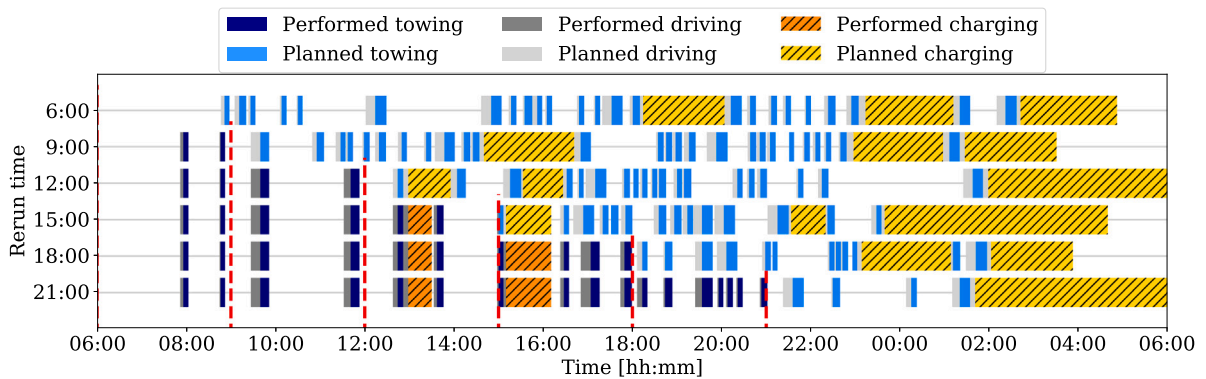
Fig. 18. Schedule evolution of one narrow-body ETV during the day, on December 14, 2019. The reevaluated schedules from 6:00 (start of the day), as well as 9:00, 12:00, 15:00, 18:00, and 21:00 are shown. For each time, the scheduled as well as actual flight arrival/departure times are used. (For interpretation of the references to color in this figure legend, the reader is referred to the web version of this article.)

7. Conclusion

This paper proposes an integrated framework to optimally dispatch a fleet of electric towing vehicles (ETVs) at a large airport. This framework integrates the routing of the ETVs in the taxiway system, where minimum separation distances are ensured at all times, with the scheduling of ETVs for towing aircraft and battery re-charging. We consider realistic ETV specifications such as battery capabilities and kinematic properties. The charging of the batteries of the ETVs follows a partial recharging policy, i.e., the charging times depend on the residual state-of-charge of the batteries. The ETV routing and task scheduling problems as posed as mixed-integer linear programs.

Our framework is illustrated for five days of operations at Amsterdam Airport Schiphol. The results show that the size of the required ETV fleet increases approximately linear with the number of flights. This ranges from a fleet of 39 ETVs to tow 896 aircraft to a fleet of 50 to tow 1258 aircraft. Our model scales for up to 2000 arriving and departing flights per day, corresponding to the busiest airports in the world. We also propose a simple greedy heuristic for the management of the ETVs. Overall, this greedy heuristic achieves an optimality gap of 5%, while decreasing the computational time by up to 97%. Finally, the robustness of the dispatchment algorithms has been compared by introducing flight delays and solving the problem using a rolling horizon framework. It was shown that the optimization algorithm is able to reevaluate the schedule such that 98.6% of the flights can still be towed, whereas the greedy heuristic is able to reallocate 95.7% of the flights.

As future work, we plan to conduct a cost–benefit analysis of the environmental impact of the size of the fleet of ETVs. We also plan to consider the impact of potential flight delays on the ETV schedule by developing a robust scheduling algorithm. Lastly, we aim to include battery properties, such as degradation and the impact of weather conditions, in the model to better reflect realistic operations. With such extensions, we aim to obtain an increasingly closer-to-implementation ETV dispatchment model.

CRediT authorship contribution statement

Simon van Oosterom: Conceptualization, Methodology, Software, Formal analysis, Investigation, Data curation, Writing – original draft, Visualization. **Mihaela Mitici:** Conceptualization, Methodology, Validation, Investigation, Writing – review & editing, Supervision, Project administration, Funding acquisition. **Jacco Hoekstra:** Writing – review & editing, Supervision.

Acknowledgment

Appendix. Overview of notation

We provide an overview of the notation used in the problem description and model formulation.

Table A.7
Overview of notation used in the problem description and formulation.

Sets		
Problem description	N_R	Runway entrance and exit nodes
	N_G	Gates
	N_X	Taxiway junctions
	N_S	Service road junctions
	E_X	Roads in the taxiway system
	E_S	Roads in the service road system
	E_X^G (E_X^R)	Roads connecting the taxiway to the gates (runways)
	E_S^G (E_S^R)	Roads connecting the service roads to the gates (runways)
	N_{CS}	ETV charging stations
	A	To-be-towed aircraft
	W	Aircraft weight classes
	$A^w \subset A$	To-be-towed aircraft of weight class w
	$A^{arr,w}$ $(A^{dep,w})$	Arriving (departing) aircraft of weight class w
MILP Phase 1	N_a	Junctions in the taxiway crossed by aircraft a
	A_n	Aircraft which cross junction $n \in N_X$
	A_n^{con}	Possible separation infringement aircraft pair
	A_{nm}^{ot}	Possible overtake aircraft pair at junction n
	A_{nm}^{ho}	Possible head-on collision aircraft pair at taxiway nm
MILP Phase 2	E_a	Taxiway roads traversed by aircraft a
	A_a^{in}	Aircraft towable before towing aircraft a
	A_a^{out}	Aircraft towable after towing aircraft a

Parameters		
General	$d_X(e)$ $(d_S(e))$	Length of taxiway (service road) e
	n^{dep}	ETV depot location
	$n^s(a)$ $(n^e(a))$	Pick-up (drop-off) location for aircraft a
	$t^s(a)$	Pick-up time for aircraft a
	$m(a)$	Mass of aircraft a
	t^{EWU} (t^{ECD})	Engine warm-up (cool-down) time
	t^{Con} (t^{DCon})	ETV connecting (de-connecting) time
	t^{PB}	Push-back time
	m_w	Mass of ETV of weight class w
	v_s	Velocity of ETVs on the service roads
	$v_{min}^w(e)$ $(v_{max}^w(e))$	Minimum (maximum) velocity of ETV from class w on road e
	a^{max}	Maximum acceleration/deceleration rate of a towed aircraft
	P_w	Energy consumption rate of ETV from class w
	P_w^c	Charging rate of ETV from class w
	α	Fast-charging threshold
	β	Slow-charging to fast-charging rate ratio
	Q_w	Battery capacity of ETV from class w
	t_{min}^c	Minimum ETV charging time
MILP Phase 1	$t_{min}^w(e)/t_{max}^w(e)$	Minimum/maximum traversing time of an aircraft of weight class w on taxiway e
	$t_{max}^{end}(a)$	Latest arrival time of aircraft a at its drop-off point
MILP Phase 2	t_e^a	Traveling time of aircraft a on taxiway e
	$t^{end}(a)$	Drop-off time of the ETV of aircraft a
	$q^X(a)$	Energy consumed by an ETV towing aircraft a
	$q_f^S(a)$	Energy consumed by an ETV driving from the depot to pick-up point of aircraft a
	$q_l^S(a)$	Energy consumed by an ETV driving from the drop-off point of aircraft a to the depot
	$q^S(a, b)$	Energy consumed by an ETV driving from the drop-off point of a to the pick-up point of b
	$q_C^S(a, b)$	Energy consumed by an ETV driving from the drop-off point of a to the pick-up point of b via the charging station
	$q_C^S(a)$	Energy consumed by an ETV driving to the pick-up point of a from the closest charging station
	$t^C(a, b)$	Time available for charging an ETV between towing a and b

Variables		
MILP Phase 1	t_n^a	Arrival time of aircraft a at junction n
	Δt_n^a	Time aircraft a takes to d_{sep} clear of junction n
	z_n^{ab}	Binary, true if aircraft a passes junction n before b
MILP Phase 2	x_{ab}	Binary, true if aircraft a is towed directly before b by the same ETV
	x_a^f	Binary, true if aircraft a is the first towed by an ETV on this day
	x_a^l	Binary, true if aircraft b is the last towed by an ETV on this day
	q_a	State of charge of the ETV which tows aircraft a at the start of towing

References

Baaren, E.v., Roling, P., 2019. Design of a zero emission aircraft towing system. In: AIAA AVIATION Forum. 17-21 June 2019, Dallas, Texas, American Institute of Aeronautics and Astronautics Inc. (AIAA), p. AIAA. http://dx.doi.org/10.2514/6.2019-2932.

Berthier, A., 2021. ACI World data reveals COVID-19's impact on world's busiest airports. https://aci.aero/2021/04/22/aci-world-data-reveals-covid-19s-impact-on-worlds-busiest-airports/.

Bräysy, O., Gendreau, M., 2005a. Vehicle routing problem with time windows, Part I: Route construction and local search algorithms. Transp. Sci. 39 (1), 104–118. http://dx.doi.org/10.1287/trsc.1030.0056.

Bräysy, O., Gendreau, M., 2005b. Vehicle routing problem with time windows, Part II: Metaheuristics. Transp. Sci. 39 (1), 119–139. http://dx.doi.org/10.1287/trsc.1030.0057.

Camillere, R., Batra, A., 2021. Assessing the environmental impact of aircraft taxiing technologies. In: 32nd Congress of the Int. Council of the Aeronautical Sciences, Vol. 9. Shanghai, China.

Chon, H.D., Agrawal, D., Abbadi, A.E., 2003. FATES: Finding a time dependent shortest path. In: Goos, G., Hartmanis, J., van Leeuwen, J., Chen, M.-S., Chrysanthis, P.K., Sloman, M., Zaslavsky, A. (Eds.), In: Mobile Data Management, vol. 2574, Springer Berlin Heidelberg, Berlin, Heidelberg, pp. 165–180. http://dx.doi.org/10.1007/3-540-36389-0_12, Series Title: Lecture Notes in Computer Science.

Conrad, R.J., Figliozzi, M.A., 2011. The recharging vehicle routing problem. In: 2011 Industrial Engineering Research Conference. IERC, URL https://web.cecs.pdx.edu/~maf/Conference_Proceedings/2011_The_Recharging_Vehicle_Routing_Problem.pdf.

Daidzic, N.E., 2017. Determination of taxiing resistances for transport category airplane tractive propulsion. Adv. Aircraft Spacecraft Sci. 4 (6), 651–677. http://dx.doi.org/10.12989/AAS.2017.4.6.651.

Desaulniers, G., Errico, F., Irnich, S., Schneider, M., 2016. Exact algorithms for electric vehicle-routing problems with time windows. Oper. Res. 64 (6), 1388–1405. http://dx.doi.org/10.1287/opre.2016.1535.

Dieke-Meier, F., Fricke, H., 2012. Expectations from a steering control transfer to cockpit crews for aircraft pushback. In: 2nd International Conference on Application and Theory of Automation in Command and Control Systems. London, pp. 62–70.

Dzikus, N., Fuchte, J., Lau, A., Gollnick, V., 2011. Potential for fuel reduction through electric taxiing. In: 11th AIAA Aviation Technology, Integration, and Operations (ATIO) Conference. American Institute of Aeronautics and Astronautics, Virginia Beach, VA, http://dx.doi.org/10.2514/6.2011-6931.

Dzikus, N.M., Wollenheit, R., Schaefer, M., Gollnick, V., 2013. The benefit of innovative taxi concepts: The impact of airport size, fleet mix and traffic growth. In: 2013 Aviation Technology, Integration, and Operations Conference. American Institute of Aeronautics and Astronautics, Los Angeles, CA, http://dx.doi.org/10.2514/6.2013-4212.

Erdoğan, S., Miller-Hooks, E., 2012. A green vehicle routing problem. Transp. Res. Part E: Logist. Transp. Rev. 48 (1), 100–114. http://dx.doi.org/10.1016/j.tre.2011.08.001.

European Commission, 2016. Paris agreement. https://ec.europa.eu/clima/eu-action/international-action-climate-change/climate-negotiations/paris-agreement_en.

Figliozzi, M.A., 2010. An iterative route construction and improvement algorithm for the vehicle routing problem with soft time windows. Transp. Res. C 18 (5), 668–679. http://dx.doi.org/10.1016/j.trc.2009.08.005.

Health, Safety and Environment office Schiphol, 2020. Schiphol Regulations. Tech. Rep, Hoofddorp, URL https://www.schiphol.nl/en/download/1640595066/43q9kGoE92CccmEeC6awa4.pdf.

Hiermann, G., Puchinger, J., Ropke, S., Hartl, R.F., 2016. The electric fleet size and mix vehicle routing problem with time windows and recharging stations. European J. Oper. Res. 252 (3), 995–1018. http://dx.doi.org/10.1016/j.ejor.2016.01.038.

IATA, 2021. Net-zero carbon emissions by 2050. https://www.iata.org/en/pressroom/2021-releases/2021-10-04-03/.

Keskin, M., Çatay, B., 2016. Partial recharge strategies for the electric vehicle routing problem with time windows. Transp. Res. C 65, 111–127. http://dx.doi.org/10.1016/j.trc.2016.01.013.

Khadilkar, H., Balakrishnan, H., 2012. Estimation of aircraft taxi fuel burn using flight data recorder archives. Transp. Res. Part D: Transp. Environ. 17 (7), 532–537. http://dx.doi.org/10.1016/j.trd.2012.06.005.

Lin, B., Ghaddar, B., Nathwani, J., 2021. Electric vehicle routing with charging/discharging under time-variant electricity prices. Transp. Res. C 130, 103285. http://dx.doi.org/10.1016/j.trc.2021.103285.

Lukic, M., Giangrande, P., Hebala, A., Nuzzo, S., Galea, M., 2019. Review, challenges, and future developments of electric taxiing systems. IEEE Trans. Transp. Electr. 5 (4), 1441–1457. http://dx.doi.org/10.1109/TTE.2019.2956862.

LVNL - Air Traffic Control the Netherlands, 2019. EHAM airport profile. https://www.lvnl.nl/eaip/2021-12-16-AIRAC/html/eAIP/EH-AD-2.EHAM-en-GB.html.

Nikoleris, T., Gupta, G., Kistler, M., 2011. Detailed estimation of fuel consumption and emissions during aircraft taxi operations at Dallas/Fort Worth International Airport. Transp. Res. Part D: Transp. Environ. 16 (4), 302–308. http://dx.doi.org/10.1016/j.trd.2011.01.007.

Omidvar, A., Tavakkoli-Moghaddam, R., 2012. Sustainable vehicle routing: Strategies for congestion management and refueling scheduling. In: 2012 IEEE International Energy Conference and Exhibition. ENERGYCON, IEEE, Florence, Italy, pp. 1089–1094. http://dx.doi.org/10.1109/EnergyCon.2012.6347732.

Ramos Pereira, M., 2019. Short-Range Route Scheduling for Electric Aircraft with Battery-Charging and Battery-Swapping Constraints (Master's thesis). Delft University of Technology, Delft, URL https://repository.tudelft.nl/islandora/object/uuid%3A94a943e9-bb73-45dd-b395-d0df6d78a95a.

Savelsbergh, M.W.P., 1992. The vehicle routing problem with time windows: Minimizing route duration. ORSA J. Comput. 4 (2), 146–154. http://dx.doi.org/10.1287/ijoc.4.2.146.

Schiphol, 2019a. Emission free by 2030. https://www.schiphol.nl/en/schiphol-as-a-neighbour/page/emission-free-by-2030/.

Schiphol, 2019b. Traffic review 2019. https://www.schiphol.nl/en/download/b2b/1586959357/2a3AhGB6ciY86vBhVbFrPW.pdf.

Schneider, M., Stenger, A., Goeke, D., 2014. The electric vehicle-routing problem with time windows and recharging stations. Transp. Sci. 48 (4), 500–520. http://dx.doi.org/10.1287/trsc.2013.0490, Publisher: INFORMS.

Shepardson, D., 2021. U.S. sets goal of net-zero aviation emissions by 2050. https://www.reuters.com/business/cop/us-sets-goal-net-zero-aviation-emissions-by-2050-2021-11-09/.

Solomon, M.M., 1987. Algorithms for the vehicle routing and scheduling problems with time window constraints. Oper. Res. 35 (2), 254–265. http://dx.doi.org/10.1287/opre.35.2.254.

Soltani, M., Ahmadi, S., Akgunduz, A., Bhuiyan, N., 2020. An eco-friendly aircraft taxiing approach with collision and conflict avoidance. Transp. Res. C 121, 102872. http://dx.doi.org/10.1016/j.trc.2020.102872.

Sydney Airport, 2021. Sydney Airport commits to net zero by 2030. https://www.sydneyairport.com.au/corporate/media/corporate-newsroom/sydney-airport-commits-to-net-zero-by-2030.

Taş, D., Dellaert, N., van Woensel, T., de Kok, T., 2014. The time-dependent vehicle routing problem with soft time windows and stochastic travel times. Transp. Res. C 48, 66–83. http://dx.doi.org/10.1016/j.trc.2014.08.007.

UNFCCC, 2021. International aviation climate ambition coalition - COP26 declaration. https://ukcop26.org/cop-26-declaration-international-aviation-climate-ambition-coalition/.